The Astrophysical Journal Supplement Series, 207:20 (10pp), 2013 August doi:10.1088/0067-0049/207/2/20

ACCURATE RITZ WAVELENGTHS OF PARITY-FORBIDDEN [Co II] AND [V II] LINES OF ASTROPHYSICAL INTEREST

M. P. Ruffoni and J. C. Pickering
Blackett Laboratory, Department of Physics, Imperial College London, London SW7 2AZ, UK; m.ruffoni@imperial.ac.uk
Received 2013 March 26; accepted 2013 May 27; published 2013 July 15

ABSTRACT

We report a comprehensive list of accurate Ritz wavelengths for parity-forbidden [Co II] and [V II] lines obtained from the analysis of energy levels measured in the laboratory with Fourier transform emission spectroscopy. Such lines, particularly those in the infrared, are in demand for the analysis of low-density astrophysical plasmas in and around objects such as planetary nebulae, star-forming regions, and active galactic nuclei. Transitions between all known metastable levels of Co II and V II are included in our analysis, producing wavelengths for 1477 [V II] lines and 782 [Co II] lines. Of these, 170 [V II] lines and 171 [Co II] lines arise from transitions with calculated transition probabilities greater than 1×10^{-2} s^{-1} and upper level excitations of less than 5 eV, and thus are likely to be observed in astrophysical spectra.

Key words: atomic data – line: profiles – methods: laboratory – techniques: spectroscopic

Online-only material: machine-readable tables

1. INTRODUCTION

Stellar spectra feature a rich array of absorption lines, generated primarily from electric dipole (E1) transitions within the atoms of a star's atmosphere. These lines may be interpreted using synthetic spectra derived from atomic and molecular line lists, and radiative processes modeled using spectra containing hundreds of millions or billions of spectroscopic transitions.

In each case though, fundamental atomic data—such as line wavelengths and identifications, transition probabilities, and line broadening parameters such as hyperfine splitting—must be known. These can be supplied on a large scale through ab initio atomic and molecular calculations, or with greater accuracy on a smaller scale through direct experimental measurements in the laboratory.

However, in recent decades, developments in astronomical spectrographs have placed greater demands on the quantity and accuracy of such data. As a result, our understanding of stellar atmospheres is frequently not limited by the quality and quantity of astronomical spectra, but by the availability of accurate atomic and molecular data with which to analyze them. This is also true of other areas of astronomical spectroscopy, which may have additional, sometimes unique, requirements.

In contrast to stellar spectra, spectra from low-density astrophysical plasmas—such as those that exist in planetary nebulae and star-forming regions, and around active galactic nuclei—also contain strong emission lines. These are generated through a number of processes, and can lead to the observation of so-called forbidden lines, which arise from the radiative de-excitation of electrons from long-lived, low-lying metastable levels. For an overview of the processes at work in nebulae and active galactic nuclei, see Osterbrock & Ferland (2006), for example.

In general, metastable levels possess the same parity as the ground state of an atom,[1] and are of lower energy than any level of opposite parity. De-excitation of electrons through E1 transitions is thus forbidden, as can be seen from the selection rules in Table 1. Electrons populating these levels must therefore de-excite through alternative mechanisms.

Higher order, magnetic dipole (M1) and electric quadrupole (E2) transitions are allowed, but for neutral and weakly ionized atoms, their transition probabilities are many orders of magnitude smaller than those for E1 transitions. As a result, in high-density plasmas—such as those that exist in stellar atmospheres or plasmas generated in the laboratory—metastable levels are predominantly de-populated through collisions with other atoms, and thus no forbidden lines are seen. However, in low-density plasmas, collisions are rare, allowing enough time for M1 and E2 transitions to occur.

Forbidden lines are thus observed in these plasmas and are important in examining different regions of planetary nebulae (Smith et al. 2005, for example) and nebulae surrounding objects such as active galactic nuclei (Meijerink et al. 2007, for example). However, it is usual for only standard pairs of forbidden lines to be used in such analyses, most commonly those from [Fe II], which is at least in part due to a lack of accurate atomic data for other forbidden lines. Barlow (2012) recently reviewed developments arising from spectroscopic studies of ionized nebulae and concluded that there is an "urgent" requirement for more atomic data of such lines; particularly so for atoms in low ionization states.

In this paper, we present a comprehensive set of accurate Ritz wavelengths for forbidden lines in Co II and V II, calculated, in each case, for transitions between all known metastable levels. These include infrared lines of astrophysical importance, some of which have already been observed in such spectra; see Fang & Liu (2011), Hartman et al. (2004), and Arkhipova et al. (2001), for example.

2. LABORATORY DATA

The Ritz wavelengths of the parity-forbidden [Co II] and [V II] lines reported here were calculated, respectively, from the accurate Co II energy levels reported by Pickering et al. (1998) and the revised accurate V II energy levels measured by Thorne et al. (2013).

[1] Exceptions include levels that are metastable to E1, M1, and E2 transitions, such as the $1s^2 2s2s^3P_2$ level in Be-like ions. In this case, decay to the $1s^2 2s^{2\,1}S_0$ involves $\Delta J = 2$ and occurs through a magnetic quadrupole (M2) transition.

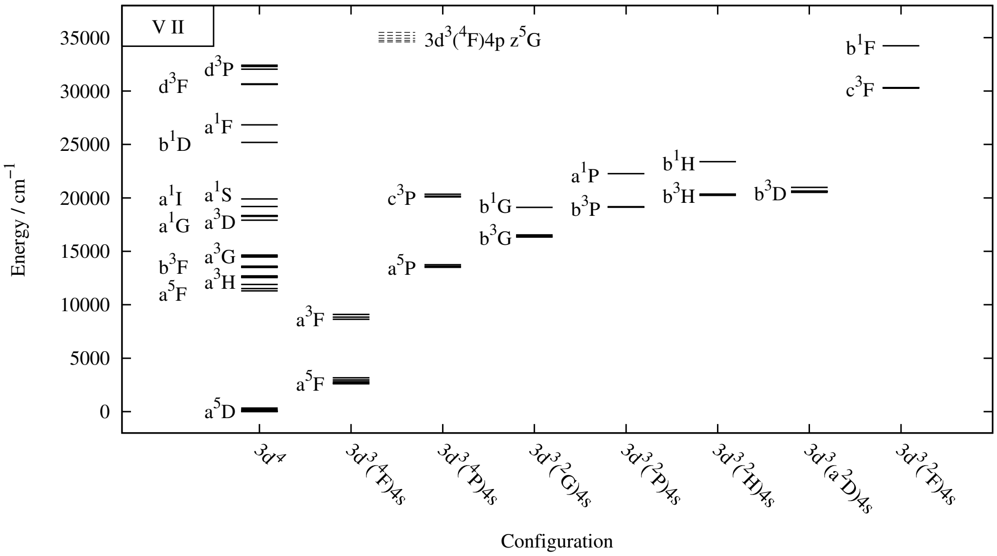

Figure 1. Energy level diagram showing the 65 known metastable levels in V II, which are of even parity. The levels belonging to the $3d^3(^4F)4p\ z^5G$ term, which is the lowest-lying term of odd parity, are also shown as dashed lines to indicate the upper limit on the region in which E1 transitions are forbidden.

In both cases, the laboratory Co II and V II spectra obtained by those researchers, and used in their spectral analyses, were generated in a water-cooled hollow cathode discharge lamp and measured on both the $f/25$ vacuum UV Fourier transform (FT) spectrometer at Imperial College London (Thorne et al. 1987) and the $f/55$ IR-visible FT spectrometer at the National Solar Observatory, Kitt Peak, Tucson, AZ (Brault 1976). Observed atomic lines were fitted using the `GREMLIN` program developed by J. W. Brault (unpublished), with care taken to account for hyperfine structure splitting by calculating a center of gravity wavenumber for each transition. The wavenumber scale was calibrated using the 26 Ar II lines recommended by Learner & Thorne (1988), and the `ELCALC` program (Radziemski & Kaufman 1969) was then used to revise the energy levels involving known transitions observed in the FT spectra. New energy levels were found using the unidentified observed lines.

The Co II spectra in Pickering et al. (1998) were wavelength calibrated using the Ar II measurements of Norlén (1973). By contrast, the V II spectra in Thorne et al. (2013) were wavelength calibrated using the more recent Ar II measurements of Whaling et al. (1995). Since the measurements of Norlén (1973) have now been superseded by those of Whaling et al. (1995), we increased the Co II energy levels of Pickering et al. (1998) by 7 parts in 10^8—the value recommended by Whaling et al. (1995)—in our calculations of [Co II] Ritz wavelengths to account for the difference between the two calibration scales. In almost all cases, however, the resulting change in line wavelength was smaller than the overall wavelength uncertainty.

3. ANALYSIS AND RESULTS

3.1. Ritz Wavelengths

V II has a complex energy level structure, with 65 metastable levels of even parity between the $3d^4\ a^5D_0$ ground state and the lowest-lying level of odd parity; the $3d^3(^4F)4p\ z^5G_2$ level at 34592.843(1) cm^{-1} (Thorne et al. 2013). These levels are shown in Figure 1, grouped by their configuration and sub-configuration, with individual spin-orbit (LS) terms labeled. The levels belonging to the lowest-lying term of odd parity are also shown to indicate the upper limit on the region in which E1 transitions are forbidden.

Table 1
Transition Rules for Allowed E1 Transitions and Parity-forbidden M1 and E2 Transitions

Transition	Parity	ΔJ	Restrictions
E1	Changes	$0, \pm1$	$(0 \nleftrightarrow 0)$
M1	No change	$0, \pm1$	$(0 \nleftrightarrow 0)$
E2	No change	$0, \pm1, \pm2$	$(0 \nleftrightarrow 0, 1/2 \nleftrightarrow 1/2, 0 \nleftrightarrow 1)$

Using the energy levels measured by Thorne et al. (2013) and the selection rules given in Table 1, we calculated accurate Ritz wavelengths for the 1477 possible parity-forbidden [V II] lines originating from M1 and E2 transitions between all 65 metastable levels. The most significant of these—those with $A \geqslant 1 \times 10^{-2}$ and upper level excitation of less than 5 eV—are listed in Table 2, with the remaining weaker lines listed in Table 4. The uncertainties in line wavelength were obtained by combining the uncertainty in the energy level value (typically 0.001 cm^{-1} to 0.003 cm^{-1}) of each of the two levels involved in a given transition.

The structure of Co II is only marginally less complex, with 47 metastable levels between the $3d^8\ a^3D_4$ ground state and the $3d^7(^4F)4p\ z^5F_5$ lowest-lying odd level at 45197.708(1) cm^{-1} (Pickering et al. 1998), as shown in Figure 2. Accurate energies for 41 of these levels are given by Pickering et al. (1998), and another five—the $3d^64s^2a^5D_1$ level and the levels belonging to the c^3F and a^1F terms of the $3d^7(^2F)4s$ configuration—by Sugar & Corliss (1985). The final metastable level, $3d^64s^2a^5D_0$, was omitted from our calculations as, to our knowledge, no experimental value exists for its energy.

By again applying the selection rules in Table 1, we calculated accurate Ritz wavelengths for the 782 possible parity-forbidden [Co II] lines originating from M1 and E2 transitions between the remaining 46 levels. The most significant lines are shown in Table 3, and the remaining weaker lines in Table 5. Where a transition takes place between levels reported by Pickering et al. (1998), the uncertainty in the Ritz wavenumber is as low as 0.001 cm^{-1}, but for those that include the levels from Sugar & Corliss (1985), this value is an order of magnitude larger due to the lower accuracy with which those energy levels are known.

Table 2
Parity-forbidden Lines in V II with a Transition Probability of At Least 1×10^{-2} s^{-1} and Upper Level Excitation Less Than 5 eV

Wavenumber	Unc.	λ_{vac}	Unc.	λ_{air}	Transition		Energy (cm^{-1})[b]		A	Type
(cm^{-1})	(cm^{-1})	(Å)	(Å)	(Å)[a]	Lower Level	Upper Level	Lower Level	Upper Level	(s^{-1})[c]	
5391.151	0.004	18548.9147	0.0124	18543.8509	a^5P_3	b^3P_2	13742	19133	1.71×10^{-2}	M1, E2
5649.623	0.004	17700.2961	0.0113	17695.4632	a^5P_1	b^3P_0	13512	19161	2.87×10^{-2}	M1
5654.515	0.004	17684.9827	0.0113	17680.1540	a^5P_1	b^3P_1	13512	19166	2.22×10^{-2}	M1, E2
7253.161	0.004	13787.0923	0.0069	13783.3234	a^3P_2	b^3P_0	11908	19161	1.02×10^{-2}	E2
7657.257	0.002	13059.5068	0.0038	13055.9357	a^3H_6	b^3H_6	12706	20363	1.99×10^{-2}	M1, E2
7658.766	0.003	13056.9337	0.0054	13053.3633	a^3H_5	b^3H_5	12621	20280	1.77×10^{-2}	M1, E2
7697.282	0.004	12991.5989	0.0061	12988.0461	a^3H_4	b^3H_4	12545	20242	1.83×10^{-2}	M1, E2
8387.824	0.004	11922.0432	0.0064	11918.7809	a^3P_1	a^1S_0	11515	19903	2.41×10^{-2}	M1
9037.817	0.004	11064.6188	0.0044	11061.5892	b^1D_2	b^1F_3	25191	34229	3.38×10^{-2}	M1, E2
9255.938	0.002	10803.8753	0.0026	10800.9164	a^3F_4	a^3D_3	9098	18354	2.05×10^{-2}	M1, E2
9427.464	0.003	10607.3065	0.0036	10604.4009	a^3F_3	a^3D_1	8842	18270	1.13×10^{-2}	E2
9629.152	0.004	10385.1305	0.0039	10382.2852	a^3F_2	a^3D_1	8640	18270	1.25×10^{-2}	M1, E2
9695.545	0.004	10314.0154	0.0045	10311.1893	b^3D_3	c^3F_4	20623	30319	1.25×10^{-2}	M1, E2
9955.193	0.004	10045.0087	0.0036	10042.2555	b^3H_6	c^3F_4	20363	30319	2.92×10^{-2}	E2
10015.040	0.001	9984.9826	0.0014	9982.2457	a^3F_4	b^1G_4	9098	19113	1.71×10^{-2}	M1, E2
10025.129	0.006	9974.9340	0.0058	9972.1998	b^3H_4	c^3F_2	20242	30268	3.26×10^{-2}	E2
10026.138	0.004	9973.9301	0.0042	9971.1963	b^3H_5	c^3F_3	20280	30306	3.11×10^{-2}	E2
10270.864	0.004	9736.2792	0.0034	9733.6098	c^3P_2	d^3F_4	20343	30614	1.27×10^{-2}	E2
10270.879	0.001	9736.2650	0.0013	9733.5955	a^3F_3	b^1G_4	8842	19113	1.04×10^{-2}	M1, E2
10521.060	0.004	9504.7457	0.0033	9502.1389	a^3F_2	b^3P_0	8640	19161	1.18×10^{-2}	E2
10525.952	0.004	9500.3283	0.0033	9497.7227	a^3F_2	b^3P_1	8640	19166	1.23×10^{-2}	M1, E2
10578.674	0.003	9452.9806	0.0025	9450.3878	a^5F_5	a^5P_3	3163	13742	1.85×10^{-2}	E2
10583.438	0.005	9448.7255	0.0048	9446.1338	c^3P_1	d^3F_2	20090	30673	1.16×10^{-2}	M1, E2
10626.334	0.004	9410.5832	0.0037	9408.0019	a^5F_4	a^5P_2	2968	13595	1.19×10^{-2}	E2
10785.764	0.004	9271.4804	0.0035	9268.9368	a^5F_3	a^5P_2	2809	13595	1.08×10^{-2}	M1, E2
10824.591	0.002	9238.2243	0.0019	9235.6897	a^5F_2	a^5P_1	2687	13512	1.23×10^{-2}	M1, E2
10837.702	0.003	9227.0483	0.0024	9224.5167	a^1H_5	b^1F_3	23391	34229	5.30×10^{-2}	E2
10906.759	0.002	9168.6265	0.0019	9166.1108	a^5F_1	a^5P_1	2605	13512	1.15×10^{-2}	M1, E2
11245.157	0.002	8892.7171	0.0018	8890.2760	a^3F_4	c^3P_2	9098	20343	1.81×10^{-2}	E2
11247.600	0.002	8890.7856	0.0018	8888.3450	a^3F_3	c^3P_1	8842	20090	1.56×10^{-2}	E2
11259.411	0.005	8881.4593	0.0042	8879.0212	a^5D_1	a^3P_0	36	11296	1.93×10^{-2}	M1
11318.330	0.007	8835.2257	0.0052	8832.8001	a^1D_2	d^3P_1	20981	32299	1.84×10^{-2}	M1, E2
11408.141	0.002	8765.6701	0.0017	8763.2633	a^5D_2	a^3P_1	107	11515	1.52×10^{-2}	M1, E2
11417.652	0.006	8758.3682	0.0045	8755.9634	b^3D_3	d^3P_2	20623	32041	6.46×10^{-2}	M1, E2
11439.123	0.010	8741.9289	0.0080	8739.5286	a^1D_2	d^3P_0	20981	32420	7.03×10^{-2}	E2
11449.288	0.003	8734.1676	0.0022	8731.7694	a^3F_2	c^3P_1	8640	20090	2.17×10^{-2}	M1, E2
11475.453	0.004	8714.2529	0.0032	8711.8601	b^3P_1	d^3F_3	19166	30642	1.44×10^{-2}	E2
11481.119	0.004	8709.9524	0.0032	8707.5607	b^3P_2	d^3F_4	19133	30614	2.58×10^{-2}	E2
11492.641	0.002	8701.2202	0.0017	8698.8309	a^5F_5	a^3G_5	3163	14656	1.37×10^{-2}	M1, E2
11500.996	0.002	8694.8991	0.0017	8692.5115	a^3F_3	c^3P_2	8842	20343	1.60×10^{-2}	M1, E2
11516.308	0.004	8683.3384	0.0027	8680.9540	a^3F_2	c^3P_0	8640	20157	3.74×10^{-2}	E2
11525.094	0.003	8676.7188	0.0024	8674.3361	a^3F_4	b^3D_3	9098	20623	1.60×10^{-2}	M1, E2
11648.390	0.003	8584.8774	0.0023	8582.5195	b^3F_3	b^1D_2	13543	25191	1.08×10^{-2}	M1, E2
11676.274	0.007	8564.3759	0.0049	8562.0236	b^3D_3	d^3P_1	20623	32299	5.62×10^{-2}	E2
11680.097	0.004	8561.5727	0.0030	8559.2212	a^3F_3	b^3D_1	8842	20522	1.51×10^{-2}	E2
11682.184	0.007	8560.0432	0.0049	8557.6921	b^3D_2	d^3P_1	20617	32299	4.01×10^{-2}	M1, E2
11697.589	0.005	8548.7702	0.0039	8546.4221	c^3P_2	d^3P_2	20343	32041	1.11×10^{-1}	M1, E2
11699.471	0.002	8547.3950	0.0016	8545.0473	a^5D_3	a^3P_2	209	11908	1.10×10^{-2}	M1, E2
11777.110	0.007	8491.0475	0.0052	8488.7150	b^3D_1	d^3P_1	20522	32299	9.32×10^{-2}	M1, E2
11802.977	0.010	8472.4388	0.0075	8470.1113	b^3D_2	d^3P_0	20617	32420	1.78×10^{-1}	E2
11881.785	0.004	8416.2439	0.0032	8413.9316	a^3F_2	b^3D_1	8640	20522	1.15×10^{-2}	M1, E2
11883.965	0.006	8414.7000	0.0041	8412.3881	c^3P_0	d^3P_2	20157	32041	3.83×10^{-2}	E2
11950.985	0.005	8367.5111	0.0038	8365.2120	c^3P_1	d^3P_2	20090	32041	1.06×10^{-1}	M1, E2
11956.211	0.006	8363.8537	0.0044	8361.5556	c^3P_2	d^3P_1	20343	32299	1.12×10^{-1}	M1, E2
12077.004	0.010	8280.1993	0.0070	8277.9238	c^3P_2	d^3P_0	20343	32420	8.69×10^{-2}	E2
12138.877	0.003	8237.9943	0.0021	8235.7303	a^3F_3	a^1D_2	8842	20981	1.86×10^{-2}	M1, E2
12209.607	0.006	8190.2718	0.0042	8188.0206	c^3P_1	d^3P_1	20090	32299	2.54×10^{-2}	M1, E2
12260.083	0.004	8156.5516	0.0024	8154.3096	a^3D_3	d^3F_4	18354	30614	2.25×10^{-2}	M1, E2
12340.565	0.004	8103.3567	0.0024	8101.1290	a^3F_2	a^1D_2	8640	20981	2.01×10^{-2}	M1, E2
12347.896	0.004	8098.5457	0.0024	8096.3193	a^3D_2	d^3F_3	18294	30642	1.65×10^{-2}	M1, E2
12379.217	0.005	8078.0553	0.0035	8075.8345	a^3D_2	d^3F_2	18294	30673	1.14×10^{-2}	M1, E2
12403.574	0.006	8062.1924	0.0038	8059.9758	a^3D_1	d^3F_2	18270	30673	1.72×10^{-2}	M1, E2
12874.321	0.006	7767.3999	0.0035	7765.2629	b^3P_1	d^3P_2	19166	32041	1.47×10^{-2}	M1, E2

Table 2
(Continued)

Wavenumber (cm^{-1})	Unc. (cm^{-1})	λ_{vac} (Å)	Unc. (Å)	λ_{air} (Å)[a]	Transition Lower Level	Transition Upper Level	Energy (cm^{-1})[b] Lower Level	Energy (cm^{-1})[b] Upper Level	A (s^{-1})[c]	Type
12907.844	0.006	7747.2272	0.0035	7745.0956	b^3P_2	d^3P_2	19133	32041	1.92×10^{-2}	M1, E2
13255.598	0.004	7543.9825	0.0023	7541.9058	a^5D_4	a^5P_2	339	13595	1.85×10^{-1}	E2
13269.814	0.001	7535.9007	0.0008	7533.8261	a^5D_4	b^3F_4	339	13609	1.31×10^{-2}	M1, E2
13287.259	0.010	7526.0067	0.0059	7523.9348	b^3P_2	d^3P_0	19133	32420	1.91×10^{-2}	E2
13303.009	0.002	7517.0963	0.0013	7515.0269	a^5D_3	a^5P_1	209	13512	2.21×10^{-1}	E2
13370.017	0.003	7479.4221	0.0016	7477.4245	a^5F_5	b^3G_5	3163	16533	2.88×10^{-2}	M1, E2
13402.515	0.002	7461.2862	0.0012	7459.2934	a^5D_4	a^5P_3	339	13742	1.76×10^{-1}	M1, E2
13405.156	0.002	7459.8162	0.0012	7457.8238	a^5D_2	a^5P_1	107	13512	1.43×10^{-1}	M1, E2
13453.139	0.001	7433.2095	0.0008	7431.2240	a^5F_4	b^3G_4	2968	16422	1.57×10^{-2}	M1, E2
13475.697	0.003	7420.7664	0.0016	7418.7842	a^5D_1	a^5P_1	36	13512	3.79×10^{-2}	M1, E2
13488.080	0.004	7413.9537	0.0023	7411.9732	a^5D_2	a^5P_2	107	13595	6.33×10^{-2}	M1, E2
13532.850	0.002	7389.4265	0.0012	7387.4525	a^5D_3	a^5P_3	209	13742	1.55×10^{-1}	M1, E2
13558.621	0.004	7375.3813	0.0024	7373.4110	a^5D_1	a^5P_2	36	13595	1.08×10^{-1}	M1, E2
13594.723	0.005	7355.7953	0.0027	7353.8301	a^5D_0	a^5P_2	0	13595	5.27×10^{-2}	E2
13634.997	0.002	7334.0684	0.0012	7332.1088	a^5D_2	a^5P_3	107	13742	7.67×10^{-2}	M1, E2
13686.808	0.005	7306.3055	0.0029	7304.3532	a^3D_3	d^3P_2	18354	32041	6.92×10^{-2}	M1, E2
13705.538	0.003	7296.3207	0.0015	7294.3710	a^5D_1	a^5P_3	36	13742	1.83×10^{-2}	E2
13746.764	0.005	7274.4393	0.0028	7272.4953	a^3D_2	d^3P_2	18294	32041	1.34×10^{-2}	M1, E2
13785.545	0.004	7253.9751	0.0019	7252.0365	b^3G_5	c^3F_4	16533	30319	8.54×10^{-2}	M1, E2
13884.861	0.003	7202.0887	0.0016	7200.1636	b^3G_4	c^3F_3	16422	30306	5.58×10^{-2}	M1, E2
13897.000	0.003	7195.7977	0.0016	7193.8743	b^3G_4	c^3F_4	16422	30319	1.38×10^{-2}	M1, E2
13926.530	0.005	7180.5396	0.0028	7178.6202	b^3G_3	c^3F_2	16341	30268	4.80×10^{-2}	M1, E2
13945.430	0.006	7170.8079	0.0033	7168.8911	a^3D_3	d^3P_1	18354	32299	5.96×10^{-2}	E2
13965.408	0.004	7160.5498	0.0018	7158.6357	b^3G_3	c^3F_3	16341	30306	1.28×10^{-2}	M1, E2
14005.386	0.006	7140.1102	0.0032	7138.2014	a^3D_2	d^3P_1	18294	32299	1.95×10^{-2}	M1, E2
14029.743	0.007	7127.7143	0.0034	7125.8087	a^3D_1	d^3P_1	18270	32299	5.60×10^{-2}	M1, E2
14080.927	0.004	7101.8052	0.0018	7099.9063	b^3G_5	d^3F_4	16533	30614	1.72×10^{-1}	M1, E2
14108.784	0.004	7087.7830	0.0018	7085.8879	b^3G_5	d^3F_3	16533	30642	3.20×10^{-2}	E2
14126.179	0.010	7079.0551	0.0051	7077.1622	a^3D_2	d^3P_0	18294	32420	1.18×10^{-1}	E2
14192.382	0.003	7046.0336	0.0016	7044.1493	b^3G_4	d^3F_4	16422	30614	3.72×10^{-2}	M1, E2
14220.239	0.003	7032.2306	0.0016	7030.3500	b^3G_4	d^3F_3	16422	30642	1.69×10^{-1}	M1, E2
14251.560	0.005	7016.7757	0.0025	7014.8991	b^3G_4	d^3F_2	16422	30673	4.87×10^{-2}	E2
14300.786	0.004	6992.6226	0.0018	6990.7523	b^3G_3	d^3F_3	16341	30642	5.43×10^{-2}	M1, E2
14332.107	0.005	6977.3412	0.0026	6975.4748	b^3G_3	d^3F_2	16341	30673	2.44×10^{-1}	M1, E2
15115.923	0.002	6615.5404	0.0010	6613.7685	b^1G_4	b^1F_3	19113	34229	5.66×10^{-2}	M1, E2
15385.438	0.002	6499.6525	0.0009	6497.9108	a^5F_4	a^3D_3	2968	18354	1.81×10^{-2}	M1, E2
15484.912	0.002	6457.8991	0.0009	6456.1683	a^5F_3	a^3D_2	2809	18294	2.64×10^{-2}	M1, E2
15582.306	0.003	6417.5354	0.0013	6415.8151	a^5F_2	a^3D_1	2687	18270	2.83×10^{-2}	M1, E2
15662.921	0.003	6384.5052	0.0013	6382.7935	a^3G_5	c^3F_4	14656	30319	1.12×10^{-2}	M1, E2
15664.474	0.003	6383.8722	0.0013	6382.1607	a^5F_1	a^3D_1	2605	18270	1.48×10^{-2}	M1, E2
15750.321	0.003	6349.0769	0.0013	6347.3745	a^3G_4	c^3F_3	14556	30306	1.63×10^{-2}	M1, E2
15805.763	0.005	6326.8062	0.0022	6325.1096	a^3G_3	c^3F_2	14462	30268	4.31×10^{-2}	M1, E2
15844.641	0.004	6311.2822	0.0014	6309.5895	a^3G_3	c^3F_3	14462	30306	1.40×10^{-2}	M1, E2
15958.303	0.003	6266.3304	0.0012	6264.6495	a^3G_5	d^3F_4	14656	30614	4.19×10^{-1}	M1, E2
15986.160	0.003	6255.4109	0.0012	6253.7329	a^3G_5	d^3F_3	14656	30642	7.37×10^{-2}	E2
16057.842	0.003	6227.4869	0.0012	6225.8161	a^3G_4	d^3F_4	14556	30614	7.60×10^{-2}	M1, E2
16085.699	0.003	6216.7022	0.0012	6215.0342	a^3G_4	d^3F_3	14556	30642	3.20×10^{-1}	M1, E2
16117.020	0.005	6204.6210	0.0020	6202.9561	a^3G_4	d^3F_2	14556	30673	9.10×10^{-2}	E2
16180.019	0.004	6180.4625	0.0014	6178.8039	a^3G_3	d^3F_3	14462	30642	8.90×10^{-2}	M1, E2
16211.340	0.005	6168.5215	0.0020	6166.8661	a^3G_3	d^3F_2	14462	30673	3.78×10^{-1}	M1, E2
16317.939	0.003	6128.2249	0.0011	6126.5799	a^1G_4	b^1F_3	17911	34229	4.78×10^{-2}	M1, E2
16348.985	0.003	6116.5877	0.0012	6114.9457	a^3F_3	b^1D_2	8842	25191	3.09×10^{-2}	M1, E2
16550.673	0.004	6042.0504	0.0013	6040.4278	a^3F_2	b^1D_2	8640	25191	1.53×10^{-2}	M1, E2
16697.450	0.003	5988.9384	0.0011	5987.3297	b^3F_4	c^3F_3	13609	30306	6.95×10^{-2}	M1, E2
16709.589	0.003	5984.5877	0.0011	5982.9800	b^3F_4	c^3F_4	13609	30319	2.45×10^{-1}	M1, E2
16724.866	0.005	5979.1211	0.0018	5977.5149	b^3F_3	c^3F_2	13543	30268	1.02×10^{-1}	M1, E2
16763.744	0.003	5965.2545	0.0011	5963.6519	b^3F_3	c^3F_3	13543	30306	1.81×10^{-1}	M1, E2
16775.883	0.003	5960.9381	0.0011	5959.3366	b^3F_3	c^3F_4	13543	30319	5.58×10^{-2}	M1, E2
16776.628	0.005	5960.6734	0.0019	5959.0720	b^3F_2	c^3F_2	13491	30268	2.33×10^{-1}	M1, E2
16815.506	0.004	5946.8921	0.0013	5945.2943	b^3F_2	c^3F_3	13491	30306	7.35×10^{-2}	M1, E2
17004.971	0.003	5880.6334	0.0011	5879.0528	b^3F_4	d^3F_4	13609	30614	5.13×10^{-2}	M1, E2
17032.828	0.003	5871.0157	0.0011	5869.4376	b^3F_4	d^3F_3	13609	30642	2.84×10^{-2}	M1, E2
17071.265	0.003	5857.7967	0.0011	5856.2220	b^3F_3	d^3F_4	13543	30614	1.31×10^{-2}	M1, E2
17099.122	0.003	5848.2535	0.0011	5846.6813	b^3F_3	d^3F_3	13543	30642	1.62×10^{-2}	M1, E2

Table 2
(Continued)

Wavenumber (cm^{-1})	Unc. (cm^{-1})	λ_{vac} (Å)	Unc. (Å)	λ_{air} (Å)[a]	Transition Lower Level	Transition Upper Level	Energy (cm^{-1})[b] Lower Level	Energy (cm^{-1})[b] Upper Level	A (s^{-1})[c]	Type
17130.443	0.005	5837.5607	0.0017	5835.9912	b^3F_3	d^3F_2	13543	30673	2.31×10^{-2}	M1, E2
17182.205	0.005	5819.9748	0.0018	5818.4099	b^3F_2	d^3F_2	13491	30673	1.45×10^{-2}	M1, E2
17654.594	0.003	5664.2481	0.0010	5662.7236	a^5F_4	b^3D_3	2968	20623	4.21×10^{-2}	M1, E2
17722.411	0.005	5642.5731	0.0017	5641.0543	a^3H_4	c^3F_2	12545	30268	3.11×10^{-2}	E2
17808.114	0.003	5615.4178	0.0010	5613.9060	a^5F_3	b^3D_2	2809	20617	3.25×10^{-2}	M1, E2
17834.939	0.004	5606.9718	0.0013	5605.4622	a^5F_2	b^3D_1	2687	20522	4.50×10^{-2}	M1, E2
17907.832	0.003	5584.1489	0.0010	5582.6452	a^3H_6	d^3F_4	12706	30614	1.18	E2
17917.107	0.004	5581.2582	0.0013	5579.7552	a^5F_1	b^3D_1	2605	20522	2.26×10^{-2}	M1, E2
17992.425	0.003	5557.8945	0.0010	5556.3976	a^3H_5	d^3F_4	12621	30614	1.27×10^{-1}	M1, E2
18020.282	0.003	5549.3027	0.0010	5547.8081	a^3H_5	d^3F_3	12621	30642	1.15	E2
18096.667	0.004	5525.8794	0.0011	5524.3909	a^3H_4	d^3F_3	12545	30642	1.58×10^{-1}	M1, E2
18127.988	0.005	5516.3320	0.0016	5514.8459	a^3H_4	d^3F_2	12545	30673	1.29	E2
18171.968	0.003	5502.9813	0.0010	5501.4986	a^5F_3	a^1D_2	2809	20981	1.71×10^{-2}	M1, E2
18398.128	0.004	5435.3356	0.0011	5433.8705	a^3P_2	c^3F_3	11908	30306	3.39×10^{-2}	M1, E2
18410.267	0.004	5431.7518	0.0011	5430.2875	a^3P_2	c^3F_4	11908	30319	9.30×10^{-2}	E2
18431.696	0.005	5425.4367	0.0015	5423.9741	b^3F_4	d^3P_2	13609	32041	1.06×10^{-1}	E2
18497.990	0.005	5405.9928	0.0015	5404.5352	b^3F_3	d^3P_2	13543	32041	2.72×10^{-2}	M1, E2
18752.727	0.005	5332.5578	0.0015	5331.1192	a^3P_1	c^3F_2	11515	30268	5.14×10^{-2}	M1, E2
18756.612	0.006	5331.4532	0.0017	5330.0150	b^3F_3	d^3P_1	13543	32299	1.01×10^{-1}	E2
18791.605	0.004	5321.5252	0.0010	5320.0895	a^3P_1	c^3F_3	11515	30306	6.96×10^{-2}	E2
18808.374	0.006	5316.7807	0.0018	5315.3462	b^3F_2	d^3P_1	13491	32299	5.01×10^{-2}	M1, E2
18929.167	0.010	5282.8526	0.0028	5281.4270	b^3F_2	d^3P_0	13491	32420	1.58×10^{-1}	E2
18971.998	0.007	5270.9261	0.0020	5269.5035	a^3P_0	c^3F_2	11296	30268	5.22×10^{-2}	E2
20132.374	0.005	4967.1241	0.0013	4965.7799	a^3P_2	d^3P_2	11908	32041	3.50×10^{-2}	M1, E2
20390.996	0.006	4904.1253	0.0015	4902.7974	a^3P_2	d^3P_1	11908	32299	7.02×10^{-2}	M1, E2
20511.789	0.010	4875.2452	0.0024	4873.9246	a^3P_2	d^3P_0	11908	32420	8.95×10^{-2}	E2
20525.851	0.005	4871.9052	0.0013	4870.5855	a^3P_1	d^3P_2	11515	32041	4.48×10^{-2}	M1, E2
20745.122	0.007	4820.4103	0.0016	4819.1039	a^3P_0	d^3P_2	11296	32041	1.99×10^{-2}	E2
20784.473	0.006	4811.2839	0.0015	4809.9798	a^3P_1	d^3P_1	11515	32299	2.30×10^{-2}	M1, E2
21208.500	0.003	4715.0906	0.0007	4713.8113	a^3F_4	c^3F_3	9098	30306	1.60×10^{-2}	M1, E2
21220.639	0.003	4712.3934	0.0007	4711.1148	a^3F_4	c^3F_4	9098	30319	4.26×10^{-2}	M1, E2
21425.461	0.005	4667.3441	0.0011	4666.0770	a^3F_3	c^3F_2	8842	30268	1.80×10^{-2}	M1, E2
21464.339	0.003	4658.8903	0.0007	4657.6253	a^3F_3	c^3F_3	8842	30306	2.73×10^{-2}	M1, E2
21516.021	0.003	4647.6995	0.0007	4646.4374	a^3F_4	d^3F_4	9098	30614	1.10×10^{-1}	M1, E2
21543.878	0.003	4641.6899	0.0007	4640.4293	a^3F_4	d^3F_3	9098	30642	2.89×10^{-2}	M1, E2
21627.149	0.005	4623.8180	0.0012	4622.5620	a^3F_2	c^3F_2	8640	30268	3.20×10^{-2}	M1, E2
21666.027	0.004	4615.5209	0.0008	4614.2671	a^3F_2	c^3F_3	8640	30306	1.07×10^{-2}	M1, E2
21771.860	0.003	4593.0848	0.0007	4591.8368	a^3F_3	d^3F_4	8842	30614	2.45×10^{-2}	M1, E2
21799.717	0.003	4587.2155	0.0007	4585.9690	a^3F_3	d^3F_3	8842	30642	8.08×10^{-2}	M1, E2
21831.038	0.005	4580.6342	0.0011	4579.3894	a^3F_3	d^3F_2	8842	30673	4.29×10^{-2}	M1, E2
22001.405	0.004	4545.1643	0.0007	4543.9285	a^3F_2	d^3F_3	8640	30642	3.16×10^{-2}	M1, E2
22032.726	0.005	4538.7030	0.0011	4537.4689	a^3F_2	d^3F_2	8640	30673	1.03×10^{-1}	M1, E2
32383.948	0.010	3087.9496	0.0010	3087.0801	a^5D_1	d^3P_0	36	32420	1.10×10^{-2}	M1

Notes.
[a] Calculated using Birch & Downs (1994) for $\lambda_{vac} > 7500$ Å, and Bönsch & Potulski (1998) for all other cases.
[b] Truncated energy. For the exact value, see Thorne et al. (2013).
[c] Calculated transition probabilities derived from the $\log(gA)$ values given by Kurucz (2006b).

(This table is also available in a machine-readable form in the online journal.)

3.2. Transition Probabilities

Also included in Tables 2–5 are calculated transition probabilities, A. In general, these were derived from the $\log(gA)$ values in Kurucz (2006a, 2006b), but for Co II, the more detailed calculations reported by Raassen et al. (1998) and Quinet (1998) were used instead, where available.

The transition probabilities of Raassen et al. (1998) were obtained through a semi-empirical method. First, the angular coefficients of the transition matrix in pure LS coupling were found using the Racah algebra, multiplied by transition integrals from a relativistic Hartree–Fock code (Parpia et al. 1996), and corrected for core polarization (Hameed 1972; Laughlin 1992). The resulting LS transition matrix was then transformed into the actual intermediate coupling by using orthogonal operators (Hansen et al. 1998); adjusting the parameters of the model Hamiltonian to yield eigenvalues as close as possible to the experimental energies of Pickering et al. (1998).

Quinet (1998) used the approximately relativistic Hartree–Fock method (Cowan & Griffin 1976), followed by a least-squares optimization of the radial parameters to reduce discrepancies between calculated energy levels and the

Table 3
Parity-forbidden Lines in Co II with a Transition Probability of At Least 1×10^{-2} s^{-1} and Upper Level Excitation Less Than 5 eV

Wavenumber (cm^{-1})	Unc. (cm^{-1})	λ_{vac} (Å)	Unc. (Å)	λ_{air} (Å)[a]	Transition Lower Level	Transition Upper Level	Energy (cm^{-1})[b] Lower Level	Energy (cm^{-1})[b] Upper Level	A (s^{-1})[c]	Type
531.801	0.001	188040.2500	0.5001	187988.9985	a^5F_4	a^5F_3	4029	4561	1.09×10^{-2}	M1
678.494	0.001	147385.2282	0.3072	147345.0570	a^5F_5	a^5F_4	3350	4029	1.24×10^{-2}	M1
895.471	0.001	111673.0670	0.1764	111642.6289	b^3F_4	b^3F_3	9813	10708	1.88×10^{-2}	M1
950.324	0.002	105227.2625	0.2476	105198.5811	a^3F_4	a^3F_3	0	950	2.24×10^{-2}	M1
1156.905	0.003	86437.5147	0.2113	86413.9543	a^3D_2	a^3D_1	28112	29269	3.17×10^{-2}	M1
1243.097	0.001	80444.2397	0.0915	80422.3125	b^3P_2	c^3P_1	24074	25318	2.65×10^{-2}	M1
1609.411	0.002	62134.5281	0.0863	62117.5908	a^1D_2	a^3P_2	11651	13261	3.08×10^{-2}	M1
1683.639	0.002	59395.1512	0.0789	59378.9604	a^1P_1	a^3D_1	27585	29269	1.49×10^{-2}	M1
1753.044	0.001	57043.6298	0.0460	57028.0798	a^1D_2	a^3P_1	11651	13404	2.87×10^{-2}	M1
2267.621	0.001	44099.0770	0.0275	44087.0542	c^3P_1	a^1P_1	25318	27585	1.18×10^{-2}	M1
2321.755	0.001	43070.8636	0.0262	43059.1210	b^1G_4	a^3H_5	25147	27469	1.49×10^{-2}	M1
2597.973	0.002	38491.5444	0.0331	38481.0495	c^3P_2	a^3D_3	24886	27484	1.18×10^{-2}	M1
2754.928	0.002	36298.5868	0.0295	36288.6893	b^1G_4	a^3H_4	25147	27902	1.72×10^{-2}	M1
3173.659	0.001	31509.3692	0.0140	31500.7764	b^3P_0	a^1P_1	24411	27585	3.94×10^{-2}	M1
3225.472	0.002	31003.2122	0.0215	30994.7573	c^3P_2	a^3D_2	24886	28112	1.68×10^{-2}	M1
3317.756	0.001	30140.8521	0.0128	30132.6321	b^3P_1	a^1P_1	24267	27585	4.23×10^{-2}	M1
3407.455	0.003	29347.4141	0.0244	29339.4102	c^3P_0	a^3D_1	25861	29269	1.89×10^{-2}	M1
3409.953	0.002	29325.9153	0.0192	29317.9173	b^3P_2	a^3D_3	24074	27484	1.31×10^{-2}	M1
3461.429	0.002	28889.8004	0.0187	28881.9212	a^3H_6	a^1H_5	27106	30567	1.11×10^{-2}	M1
3510.718	0.001	28484.1998	0.0115	28476.4310	b^3P_2	a^1P_1	24074	27585	2.87×10^{-2}	M1
3522.704	0.001	28387.2823	0.0114	28379.5399	a^3G_5	b^1G_4	21625	25147	1.41×10^{-2}	M1
3614.274	0.002	27668.0719	0.0171	27660.5254	a^1P_1	b^1D_2	27585	31199	1.97×10^{-2}	M1
3715.039	0.003	26917.6159	0.0205	26910.2738	a^3D_3	b^1D_2	27484	31199	3.20×10^{-2}	M1
3951.260	0.002	25308.3809	0.0143	25301.4770	c^3P_1	a^3D_1	25318	29269	7.19×10^{-2}	M1
4037.452	0.002	24768.0946	0.0137	24761.3378	b^3P_2	a^3D_2	24074	28112	2.20×10^{-2}	M1
4382.377	0.002	22818.6651	0.0116	22812.4391	c^3P_2	a^3D_1	24886	29269	6.44×10^{-2}	M1
4857.298	0.002	20587.5763	0.0095	20581.9576	b^3P_0	a^3D_1	24411	29269	1.52×10^{-2}	M1
5481.215	0.002	18244.1289	0.0074	18239.1480	a^3G_5	a^3H_6	21625	27106	3.80×10^{-2}	M1
5487.730	0.002	18222.4696	0.0074	18217.4946	a^3G_3	a^3H_4	22414	27902	2.85×10^{-2}	M1
5844.459	0.001	17110.2223	0.0041	17105.5500	a^3G_5	a^3H_5	21625	27469	3.87×10^{-2}	M1
5892.816	0.002	16969.8143	0.0064	16965.1801	a^3G_4	a^3H_4	22009	27902	6.87×10^{-2}	M1
5928.741	0.002	16866.9863	0.0064	16862.3800	a^5P_1	b^3P_1	18339	24267	4.20×10^{-2}	M1
6072.838	0.002	16466.7645	0.0061	16462.2671	a^5P_1	b^3P_0	18339	24411	6.94×10^{-2}	M1
6117.161	0.001	16347.4515	0.0038	16342.9866	a^5F_1	b^3F_2	5205	11322	1.35×10^{-2}	M1
6302.912	0.001	15865.6813	0.0036	15861.3474	a^5P_3	b^3P_2	17772	24074	1.61×10^{-2}	M1
6313.012	0.002	15840.2983	0.0056	15835.9713	c^3P_2	b^1D_2	24886	31199	1.61×10^{-1}	M1
6462.365	0.001	15474.2100	0.0034	15469.9825	a^5F_5	b^3F_4	3350	9813	2.81×10^{-2}	M1
6547.759	0.002	15272.3998	0.0052	15268.2272	a^5P_1	c^3P_2	18339	24886	1.87×10^{-2}	M1
6854.972	0.001	14587.9506	0.0030	14583.9641	a^5P_2	c^3P_2	18031	24886	9.26×10^{-2}	M1
6932.030	0.002	14425.7877	0.0047	14421.8453	b^3P_1	b^1D_2	24267	31199	2.56×10^{-2}	M1
6978.876	0.002	14328.9540	0.0046	14325.0379	a^5P_1	c^3P_1	18339	25318	1.33×10^{-1}	M1
7114.892	0.001	14055.0261	0.0028	14051.1845	a^5P_3	c^3P_2	17772	24886	1.68×10^{-1}	M1
7522.682	0.003	13293.1322	0.0050	13289.4976	a^5P_1	c^3P_0	18339	25861	1.35×10^{-1}	M1
8557.829	0.001	11685.2072	0.0019	11682.0092	a^3G_4	a^1H_5	22009	30567	4.33×10^{-2}	M1
8942.645	0.001	11182.3744	0.0018	11179.3128	a^3G_5	a^1H_5	21625	30567	1.05×10^{-1}	M1
9246.498	0.002	10814.9057	0.0026	10811.9438	a^5P_1	a^1P_1	18339	27585	2.04×10^{-2}	M1
9452.946	0.002	10578.7131	0.0025	10575.8153	a^5P_2	a^3D_3	18031	27484	1.65×10^{-2}	M1
9712.866	0.002	10295.6227	0.0024	10292.8016	a^5P_3	a^3D_3	17772	27484	5.69×10^{-2}	M1
9724.663	0.002	10283.1330	0.0024	10280.3153	a^3F_2	b^3F_2	1597	11322	2.69×10^{-2}	M1, E2
9758.007	0.002	10247.9946	0.0023	10245.1865	a^3F_3	b^3F_3	950	10708	2.25×10^{-2}	E2
9773.232	0.003	10232.0300	0.0030	10229.2262	a^5P_1	a^3D_2	18339	28112	1.21×10^{-2}	M1
9812.860	0.001	10190.7093	0.0015	10187.9166	a^3F_4	b^3F_4	0	9813	3.43×10^{-2}	E2
10054.080	0.002	9946.2112	0.0022	9943.4848	a^3F_2	a^1D_2	1597	11651	7.91×10^{-2}	M1, E2
10080.445	0.002	9920.1973	0.0022	9917.4779	a^5P_2	a^3D_2	18031	28112	4.37×10^{-2}	M1
10371.536	0.002	9641.7737	0.0021	9639.1298	a^3F_3	b^3F_2	950	11322	2.02×10^{-2}	M1, E2
10700.953	0.002	9344.9623	0.0020	9342.3988	a^3F_3	a^1D_2	950	11651	1.71×10^{-1}	M1
10708.331	0.001	9338.5237	0.0012	9335.9619	a^3F_4	b^3F_3	0	10708	1.51×10^{-2}	E2
10863.061	0.001	9205.5087	0.0012	9202.9829	a^3P_1	b^3P_1	13404	24267	1.18×10^{-2}	E2
11006.694	0.002	9085.3804	0.0018	9082.8872	a^3P_2	b^3P_1	13261	24267	2.33×10^{-2}	E2
11092.571	0.001	9015.0428	0.0011	9012.5686	b^3F_2	a^3G_3	11322	22414	2.39×10^{-2}	M1
11150.791	0.002	8967.9738	0.0018	8965.5124	a^3P_2	b^3P_0	13261	24411	4.62×10^{-2}	E2
11482.079	0.001	8709.2243	0.0011	8706.8328	a^3P_1	c^3P_2	13404	24886	1.88×10^{-2}	E2
11593.446	0.001	8625.5632	0.0011	8623.1944	a^1G_4	a^1H_5	18974	30567	8.28×10^{-2}	E2

Table 3
(Continued)

Wavenumber (cm^{-1})	Unc. (cm^{-1})	λ_{vac} (Å)	Unc. (Å)	λ_{air} (Å)[a]	Transition Lower Level	Transition Upper Level	Energy (cm^{-1})[b] Lower Level	Energy (cm^{-1})[b] Upper Level	A (s^{-1})[c]	Type
11625.712	0.002	8601.6238	0.0017	8599.2615	a^3P_2	c^3P_2	13261	24886	1.18×10^{-2}	E2
11663.491	0.003	8573.7625	0.0021	8571.4076	a^3F_2	a^3P_2	1597	13261	1.75×10^{-2}	M1
11706.100	0.001	8542.5549	0.0010	8540.2085	b^3F_3	a^3G_3	10708	22414	3.93×10^{-2}	M1
11811.669	0.001	8466.2042	0.0010	8463.8784	b^3F_4	a^3G_5	9813	21625	3.78×10^{-2}	M1
11996.091	0.004	8336.0489	0.0025	8333.7583	a^3F_2	a^3P_0	1597	13593	3.11×10^{-2}	E2
12196.485	0.001	8199.0837	0.0010	8196.8301	b^3F_4	a^3G_4	9813	22009	4.85×10^{-2}	M1
12310.364	0.003	8123.2367	0.0019	8121.0037	a^3F_3	a^3P_2	950	13261	6.77×10^{-2}	M1, E2
12453.997	0.002	8029.5508	0.0014	8027.3430	a^3F_3	a^3P_1	950	13404	2.45×10^{-2}	E2
12616.105	0.001	7926.3767	0.0009	7924.1968	a^1D_2	b^3P_1	11651	24267	4.20×10^{-2}	E2
12760.202	0.001	7836.8666	0.0009	7834.7108	a^1D_2	b^3P_0	11651	24411	4.12×10^{-2}	E2
12945.522	0.001	7724.6789	0.0008	7722.5534	b^3F_2	b^3P_1	11322	24267	1.52×10^{-2}	E2
13089.619	0.001	7639.6418	0.0008	7637.5393	b^3F_2	b^3P_0	11322	24411	2.12×10^{-2}	E2
13133.942	0.002	7613.8604	0.0013	7611.7648	a^5F_1	a^5P_1	5205	18339	1.23×10^{-2}	E2
13235.123	0.001	7555.6533	0.0008	7553.5734	a^1D_2	c^3P_2	11651	24886	1.90×10^{-2}	M1, E2
13260.688	0.002	7541.0869	0.0013	7539.0110	a^3F_4	a^3P_2	0	13261	2.80×10^{-2}	E2
13388.578	0.002	7469.0531	0.0012	7467.0583	a^5F_2	a^5P_1	4950	18339	1.50×10^{-2}	E2
13470.638	0.001	7423.5534	0.0008	7421.5705	a^5F_3	a^5P_2	4561	18031	1.39×10^{-2}	E2
13495.956	0.001	7409.6270	0.0008	7407.6477	a^1D_2	b^1G_4	11651	25147	5.39×10^{-2}	E2
13559.051	0.001	7375.1474	0.0008	7373.1772	b^3F_3	b^3P_1	10708	24267	2.35×10^{-2}	E2
13564.540	0.001	7372.1630	0.0008	7370.1935	b^3F_2	c^3P_2	11322	24886	1.81×10^{-2}	M1
13742.519	0.001	7276.6863	0.0007	7274.7418	a^5F_4	a^5P_3	4029	17772	1.05×10^{-2}	E2
13777.851	0.002	7258.0260	0.0012	7256.0863	a^5F_3	a^5P_1	4561	18339	1.04×10^{-2}	E2
14002.439	0.001	7141.6130	0.0007	7139.7037	a^5F_4	a^5P_2	4029	18031	2.00×10^{-2}	E2
14178.069	0.001	7053.1467	0.0007	7051.2605	b^3F_3	c^3P_2	10708	24886	1.03×10^{-2}	M1, E2
14180.817	0.001	7051.7799	0.0007	7049.8941	a^3P_1	a^1P_1	13404	27585	2.02×10^{-2}	M1, E2
14223.685	0.003	7030.5269	0.0014	7028.6467	a^3P_2	a^3D_3	13261	27484	1.07×10^{-2}	M1, E2
14261.560	0.001	7011.8556	0.0007	7009.9803	b^3F_4	b^3P_2	9813	24074	2.61×10^{-2}	E2
14324.450	0.002	6981.0708	0.0011	6979.2035	a^3P_2	a^1P_1	13261	27585	4.70×10^{-2}	E2
14421.013	0.001	6934.3256	0.0007	6932.4705	a^5F_5	a^5P_3	3350	17772	3.68×10^{-2}	E2
14438.902	0.001	6925.7344	0.0007	6923.8815	b^3F_3	b^1G_4	10708	25147	1.11×10^{-1}	M1
14851.184	0.003	6733.4699	0.0013	6731.6672	a^3P_2	a^3D_2	13261	28112	1.53×10^{-2}	E2
15073.540	0.001	6634.1417	0.0006	6632.3649	b^3F_4	c^3P_2	9813	24886	1.65×10^{-2}	E2
15334.373	0.001	6521.2969	0.0006	6519.5496	b^3F_4	b^1G_4	9813	25147	1.93×10^{-1}	M1
15933.861	0.001	6275.9427	0.0006	6274.2593	a^1D_2	a^1P_1	11651	27585	1.31×10^{-1}	E2
16008.089	0.003	6246.8418	0.0011	6245.1659	a^3P_2	a^3D_1	13261	29269	1.16×10^{-1}	E2
16250.884	0.002	6153.5114	0.0008	6151.8598	a^1D_2	a^3H_4	11651	27902	1.14×10^{-2}	E2
16263.278	0.001	6148.8219	0.0005	6147.1715	b^3F_2	a^1P_1	11322	27585	2.52×10^{-2}	M1
16776.042	0.002	5960.8815	0.0008	5959.2801	b^3F_3	a^3D_3	10708	27484	6.83×10^{-2}	M1
16790.012	0.002	5955.9218	0.0008	5954.3217	b^3F_2	a^3D_2	11322	28112	3.42×10^{-2}	M1
17376.530	0.002	5754.8889	0.0007	5753.3409	a^3F_2	a^1G_4	1597	18974	3.76×10^{-2}*	E2
17403.541	0.002	5745.9570	0.0007	5744.4114	b^3F_3	a^3D_2	10708	28112	1.34×10^{-2}	M1
17448.555	0.001	5731.1335	0.0005	5729.5917	a^5F_3	a^3G_4	4561	22009	9.63×10^{-2}	M1
17464.368	0.001	5725.9443	0.0005	5724.4039	a^5F_2	a^3G_3	4950	22414	6.65×10^{-2}	M1
17595.540	0.001	5683.2583	0.0005	5681.7289	a^5F_4	a^3G_5	4029	21625	7.93×10^{-2}	M1
17617.500	0.002	5676.1742	0.0007	5674.6466	a^1D_2	a^3D_1	11651	29269	1.96×10^{-1}	E2
17671.513	0.002	5658.8249	0.0007	5657.3019	b^3F_4	a^3D_3	9813	27484	1.19×10^{-1}	M1
17853.641	0.001	5601.0983	0.0004	5599.5902	a^5F_3	a^3G_3	4561	22414	8.70×10^{-2}	M1
17938.724	0.003	5574.5324	0.0009	5573.0312	a^3P_2	b^1D_2	13261	31199	1.63×10^{-1}	E2
17946.917	0.002	5571.9876	0.0007	5570.4870	b^3F_2	a^3D_1	11322	29269	4.76×10^{-2}	M1, E2
17980.356	0.001	5561.6251	0.0004	5560.1272	a^5F_4	a^3G_4	4029	22009	2.20×10^{-1}	M1
18023.403	0.002	5548.3417	0.0007	5546.8473	a^3F_3	a^1G_4	950	18974	7.09×10^{-2}	M1
18274.034	0.001	5472.2454	0.0004	5470.7707	a^5F_5	a^3G_5	3350	21625	3.92×10^{-1}	M1
18385.442	0.001	5439.0859	0.0004	5437.6198	a^5F_4	a^3G_3	4029	22414	1.45×10^{-2}	M1
18658.850	0.001	5359.3870	0.0004	5357.9415	a^5F_5	a^3G_4	3350	22009	2.33×10^{-2}	M1
18973.727	0.001	5270.4457	0.0004	5269.0232	a^3F_4	a^1G_4	0	18974	1.38×10^{-1}	M1
19513.630	0.001	5124.6231	0.0004	5123.2382	a^5F_3	b^3P_2	4561	24074	1.69×10^{-2}	M1
19548.135	0.002	5115.5774	0.0006	5114.1949	a^1D_2	b^1D_2	11651	31199	7.10×10^{-1}	M1, E2
19877.552	0.002	5030.8005	0.0006	5029.4399	b^3F_2	b^1D_2	11322	31199	3.23×10^{-1}	M1, E2
20112.818	0.001	4971.9536	0.0003	4970.6082	a^5F_1	c^3P_1	5205	25318	2.28×10^{-2}	M1
20325.610	0.001	4919.9014	0.0003	4918.5694	a^5F_3	c^3P_2	4561	24886	3.03×10^{-2}	M1
20367.454	0.001	4909.7937	0.0003	4908.4643	a^5F_2	c^3P_1	4950	25318	2.81×10^{-2}	M1
20412.147	0.002	4899.0436	0.0005	4897.7169	a^3F_2	a^3G_4	1597	22009	2.84×10^{-2}	E2
20491.081	0.002	4880.1719	0.0005	4878.8501	b^3F_3	b^1D_2	10708	31199	5.83×10^{-1}	M1

Table 3
(Continued)

Wavenumber (cm^{-1})	Unc. (cm^{-1})	λ_{vac} (Å)	Unc. (Å)	λ_{air} (Å)[a]	Transition Lower Level	Transition Upper Level	Energy (cm^{-1})[b] Lower Level	Energy (cm^{-1})[b] Upper Level	A (s^{-1})[c]	Type
20674.204	0.002	4836.9455	0.0005	4835.6348	a^3F_3	a^3G_5	950	21625	2.56×10^{-2}	E2
20817.233	0.002	4803.7123	0.0005	4802.4101	a^3F_2	a^3G_3	1597	22414	4.41×10^{-1}	E2
21059.020	0.002	4748.5589	0.0005	4747.2710	a^3F_3	a^3G_4	950	22009	4.64×10^{-1}	E2
21464.107	0.002	4658.9407	0.0005	4657.6758	a^3F_3	a^3G_3	950	22414	1.26×10^{-1}	E2
21624.529	0.001	4624.3783	0.0003	4623.1222	a^3F_4	a^3G_5	0	21625	6.38×10^{-1}	E2
22009.345	0.001	4543.5247	0.0003	4542.2893	a^3F_4	a^3G_4	0	22009	1.03×10^{-1}	E2
22380.440	0.001	4468.1875	0.0003	4466.9714	a^5F_1	a^1P_1	5205	27585	1.61×10^{-1}	M1
22477.223	0.002	4448.9482	0.0004	4447.7371	a^3F_2	b^3P_2	1597	24074	2.96×10^{-2}	E2
22534.311	0.002	4437.6774	0.0004	4436.4691	a^5F_2	a^3D_3	4950	27484	2.91×10^{-2}	M1
22635.076	0.001	4417.9221	0.0003	4416.7189	a^5F_2	a^1P_1	4950	27585	3.48×10^{-1}	M1
22670.185	0.002	4411.0801	0.0004	4409.8786	a^3F_2	b^3P_1	1597	24267	3.19×10^{-1}	E2
22814.282	0.002	4383.2193	0.0004	4382.0250	a^3F_2	b^3P_0	1597	24411	4.14×10^{-1}	E2
22907.174	0.002	4365.4447	0.0004	4364.2549	a^5F_1	a^3D_2	5205	28112	7.17×10^{-2}	M1
22923.584	0.002	4362.3197	0.0004	4361.1307	a^5F_3	a^3D_3	4561	27484	1.31×10^{-2}	M1
23124.096	0.002	4324.4934	0.0004	4323.3141	a^3F_3	b^3P_2	950	24074	3.58×10^{-1}	E2
23161.810	0.002	4317.4519	0.0004	4316.2744	a^5F_2	a^3D_2	4950	28112	6.63×10^{-2}	M1
23317.058	0.002	4288.7058	0.0004	4287.5356	a^3F_3	b^3P_1	950	24267	4.65×10^{-1}	E2
23455.385	0.002	4263.4133	0.0004	4262.2496	a^5F_4	a^3D_3	4029	27484	5.91×10^{-1}	M1
23550.036	0.002	4246.2781	0.0004	4245.1187	a^3F_2	b^1G_4	1597	25147	9.41×10^{-2}	E2
23551.083	0.002	4246.0893	0.0004	4244.9299	a^5F_3	a^3D_2	4561	28112	7.62×10^{-1}	M1
23720.320	0.002	4215.7948	0.0004	4214.6432	a^3F_2	c^3P_1	1597	25318	3.75×10^{-1}	E2
24064.079	0.002	4155.5715	0.0004	4154.4352	a^5F_1	a^3D_1	5205	29269	1.74×10^{-1}	M1
24074.420	0.001	4153.7865	0.0002	4152.6507	a^3F_4	b^3P_2	0	24074	2.41	E2
24264.125	0.003	4121.3108	0.0005	4120.1832	a^3F_2	c^3P_0	1597	25861	2.46	E2
24318.715	0.002	4112.0594	0.0004	4110.9342	a^5F_2	a^3D_1	4950	29269	3.71×10^{-1}	M1
24367.193	0.002	4103.8786	0.0004	4102.7554	a^3F_3	c^3P_1	950	25318	1.65	E2
24886.400	0.001	4018.2590	0.0002	4017.1576	a^3F_4	c^3P_2	0	24886	3.88×10^{-2}	E2
25147.233	0.001	3976.5807	0.0002	3975.4898	a^3F_4	b^1G_4	0	25147	1.29×10^{-2}	M1, E2
25887.176	0.003	3862.9166	0.0004	3861.8544	a^3F_2	a^3D_3	1597	27484	3.74×10^{-2}	E2
25987.941	0.002	3847.9386	0.0003	3846.8802	a^3F_2	a^1P_1	1597	27585	4.94×10^{-1}	E2
26304.964	0.003	3801.5639	0.0004	3800.5172	a^3F_2	a^3H_4	1597	27902	1.50	E2
26514.675	0.003	3771.4964	0.0004	3770.4573	a^3F_2	a^3D_2	1597	28112	5.27×10^{-1}	E2
26518.664	0.002	3770.9291	0.0003	3769.8901	a^3F_3	a^3H_5	950	27469	1.73	E2
26534.049	0.003	3768.7426	0.0004	3767.7042	a^3F_3	a^3D_3	950	27484	3.84×10^{-1}	E2
26634.814	0.002	3754.4847	0.0003	3753.4498	a^3F_3	a^1P_1	950	27585	2.71×10^{-1}	E2
26951.837	0.003	3710.3222	0.0004	3709.2985	a^3F_3	a^3H_4	950	27902	1.40×10^{-1}	E2
27105.744	0.002	3689.2550	0.0003	3688.2365	a^3F_4	a^3H_6	0	27106	2.06	E2
27161.548	0.003	3681.6753	0.0004	3680.6588	a^3F_3	a^3D_2	950	28112	1.06	E2
27468.988	0.001	3640.4690	0.0002	3639.4628	a^3F_4	a^3H_5	0	27469	1.05×10^{-1}	E2
27484.373	0.002	3638.4312	0.0003	3637.4255	a^3F_4	a^3D_3	0	27484	1.35	E2
27671.580	0.003	3613.8161	0.0004	3612.8165	a^3F_2	a^3D_1	1597	29269	8.69×10^{-1}	E2
28111.872	0.002	3557.2160	0.0003	3556.2306	a^3F_4	a^3D_2	0	28112	9.09×10^{-2}	E2
28318.453	0.003	3531.2663	0.0004	3530.2874	a^3F_3	a^3D_1	950	29269	4.61×10^{-2}	E2
29616.849	0.002	3376.4564	0.0003	3375.5160	a^3F_3	a^1H_5	950	30567	4.39×10^{-2}	E2
30249.088	0.003	3305.8848	0.0003	3304.9618	a^3F_3	b^1D_2	950	31199	1.50×10^{-2}	M1, E2

Notes.
[a] Calculated using Birch & Downs (1994) for $\lambda_{vac} > 7500$ Å, and Bönsch & Potulski (1998) for all other cases.
[b] Truncated energy. For the exact value, scale the energies given in Pickering et al. (1998) by 7 parts in 10^8.
[c] Calculated transition probabilities taken from Raassen et al. (1998). The line at 17376.531 cm^{-1} (*) is not given by Raassen et al. (1998), so the value shown is from Quinet (1998).

(This table is also available in a machine-readable form in the online journal.)

experimental levels reported by Sugar & Corliss (1985). Quinet (1998) also noted that strong multiplets are typically composed of only one type of transition; M1 transitions being dominant for inter-combination multiplets ($\Delta S \neq 0$) and E2 transitions dominating under LS-coupled selection rules ($\Delta S = 0$).

A comparison of the transition probabilities obtained by Raassen et al. (1998), A_R, with those obtained by Quinet (1998), A_Q, is shown in Figure 3. Here, it can be seen that for the majority of lines, A_R and A_Q differ by no more than about 25%, although at values of A_R less than 0.1 s^{-1}, there is a significant minority of lines where differences increase to around a factor of two. At higher values of A_R, the two sets of results converge, but rather than approaching zero difference, there is a systematic difference; A_Q being approximately 25% larger than A_R at values of A_R greater than 0.1 s^{-1}.

Table 4
Parity-forbidden Lines in V II with a Transition Probability Less Than 1×10^{-2} s^{-1} or Upper Level Excitation Greater Than 5 eV

Wavenumber (cm^{-1})	Unc. (cm^{-1})	λ_{vac} (Å)	Unc. (Å)	λ_{air} (Å)[a]	Transition Lower Level	Transition Upper Level	Energy (cm^{-1})[b] Lower Level	Energy (cm^{-1})[b] Upper Level	A (s^{-1})[c]	Type
4.892	0.004	20441537.2036	17728.1475	20435965.8233	b^3P_0	b^3P_1	19161	19166	1.79×10^{-9}	M1
5.910	0.004	16920473.7733	12146.7835	16915862.0656	b^3D_2	b^3D_3	20617	20623	2.29×10^{-9}	M1, E2
12.139	0.004	8237910.8658	2879.1907	8235665.6073	c^3F_3	c^3F_4	30306	30319	3.62×10^{-8}	M1, E2
14.216	0.004	7034327.5183	2040.1854	7032410.2988	a^5P_2	b^3F_4	13595	13609	1.17×10^{-18}	E2
19.862	0.003	5034739.7040	801.5932	5033367.4759	b^1G_4	b^3P_2	19113	19133	3.80×10^{-19}	E2
20.916	0.003	4781028.8774	646.5286	4779725.7988	b^3F_2	a^5P_1	13491	13512	2.43×10^{-18}	E2
24.357	0.004	4105595.9272	607.7488	4104476.9391	a^3D_1	a^3D_2	18270	18294	3.14×10^{-7}	M1, E2
27.857	0.004	3589761.9988	546.7233	3588783.6022	d^3F_4	d^3F_3	30614	30642	5.57×10^{-7}	M1, E2
28.631	0.004	3492717.6836	517.5630	3491765.7367	b^3P_2	b^3P_0	19133	19161	5.03×10^{-16}	E2
30.846	0.002	3241911.4310	235.0105	3241027.8417	a^5P_1	b^3F_3	13512	13543	1.79×10^{-17}	E2

Notes.
[a] Calculated using Birch & Downs (1994) for $\lambda_{vac} > 7500$ Å, and Bönsch & Potulski (1998) for all other cases.
[b] Truncated energy. For the exact value, see Thorne et al. (2013).
[c] Calculated transition probabilities derived from the log(gA) values given by Kurucz (2006b).

(This table is available in its entirety in a machine-readable form in the online journal. A portion is shown here for guidance regarding its form and content.)

Table 5
Parity-forbidden Lines in Co II with a Transition Probability Less Than 1×10^{-2} s^{-1} or Upper Level Excitation Greater Than 5 eV

Wavenumber (cm^{-1})	Unc. (cm^{-1})	λ_{vac} (Å)	Unc. (Å)	λ_{air} (Å)[a]	Transition Lower Level	Transition Upper Level	Energy (cm^{-1})[b] Lower Level	Energy (cm^{-1})[b] Upper Level	A (s^{-1})[c]	Type
15.385	0.002	6499837.0491	944.6914	6498065.5060	a^3H_5	a^3D_3	27469	27484	2.03×10^{-20}	E2
76.085	0.031	1314319.4191	536.3402	1313961.1987	a^5D_4	c^3F_2	40695	40771		
100.765	0.002	992408.0087	22.0224	992137.5259	a^3D_3	a^1P_1	27484	27585	4.86×10^{-17}	E2
108.330	0.042	923105.2617	361.5253	922853.6674	c^3F_2	c^3F_3	40771	40879	3.28×10^{-5}	M1, E2
143.633	0.002	696218.7868	10.8387	696029.0308	a^3P_2	a^3P_1	13261	13404	5.18×10^{-5}	M1, E2
144.097	0.001	693976.9253	6.8109	693787.7803	b^3P_1	b^3P_0	24267	24411	1.44×10^{-4}	M1
167.620	0.042	596587.4776	151.0026	596424.8763	c^3F_3	c^3F_4	40879	41047	9.50×10^{-5}	M1, E2
184.415	0.031	542255.2016	91.2948	542107.4086	a^5D_4	c^3F_3	40695	40879	4.78×10^{-9}	M1, E2
188.967	0.003	529192.8908	8.8558	529048.6580	a^3P_1	a^3P_0	13404	13593	3.64×10^{-4}	M1
192.962	0.001	518236.7150	3.7981	518095.4683	b^3P_2	b^3P_1	24074	24267	8.14×10^{-5}	M1, E2

Notes.
[a] Calculated using Birch & Downs (1994) for $\lambda_{vac} > 7500$ Å, and Bönsch & Potulski (1998) for all other cases.
[b] Truncated energy. For the exact value, scale the energies given in Pickering et al. (1998) by 7 parts in 10^8.
[c] Calculated transition probabilities of 1×10^{-3} or greater were taken from Raassen et al. (1998) unless marked with a * or †. Values less than 1×10^{-3} were derived from the log(gA) values given by Kurucz (2006b).
* Transition probability greater than 1×10^{-3} taken from Quinet (1998).
† Transition probability greater than 1×10^{-3} derived from the log(gA) values given by Kurucz (2006b).

(This table is available in its entirety in a machine-readable form in the online journal. A portion is shown here for guidance regarding its form and content.)

In this paper, we choose to adopt the values given by Raassen et al. (1998), where possible, as these authors employed the more accurate and new energy levels of Pickering et al. (1998) in their calculations. We therefore only include values from Quinet (1998) in Tables 3 and 5 where no corresponding value is available in Raassen et al. (1998). If neither author reports a transition probability for a given line, as is the case for $A < 1 \times 10^{-3}$ s^{-1}, the transition probability shown in Tables 3 and 5 is derived from the log(gA) values in Kurucz (2006b).

3.3. Air Wavelengths

In addition to the vacuum Ritz wavelengths for [V II] and [Co II] lines, Tables 2–5 also list the calculated air wavelength of each line, λ_{air}. Aldenius & Johansson (2007) give a detailed review of approaches to calculating λ_{air} in different spectral regions. Following their approach, the refractive index correction given by Birch & Downs (1994) was used for lines in the infrared ($\lambda_{vac} > 7500$ Å). For all lines of shorter wavelength, the correction given by Bönsch & Potulski (1998) was used.

4. SUMMARY

We have presented a comprehensive list of accurate Ritz wavelengths for parity-forbidden [Co II] and [V II] lines, calculated by considering radiative M1 and E2 transitions between all known metastable levels in each species. These data will aid the analysis of spectra from low-density astrophysical plasmas, particularly in the infrared where strong forbidden lines are seen in both the near-IR, from transitions between LS terms, and far-IR, from transitions between fine-structure levels.

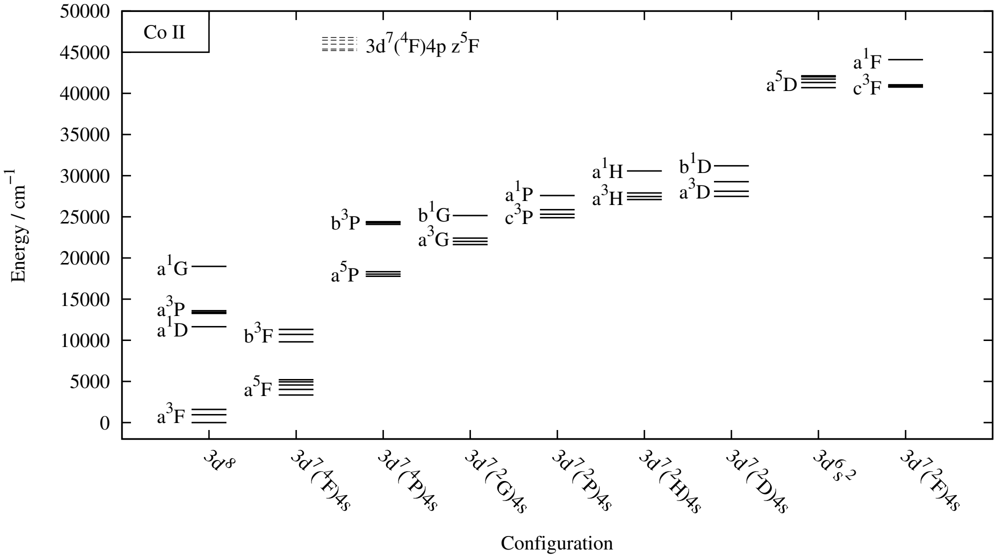

Figure 2. Energy level diagram showing the 47 known metastable levels in Co II, which are of even parity. The levels belonging to the $3d^7(^4F)4pz^5F$ term, which is the lowest-lying term of odd parity, are also shown as dashed lines to indicate the upper limit on the region in which E1 transitions are forbidden.

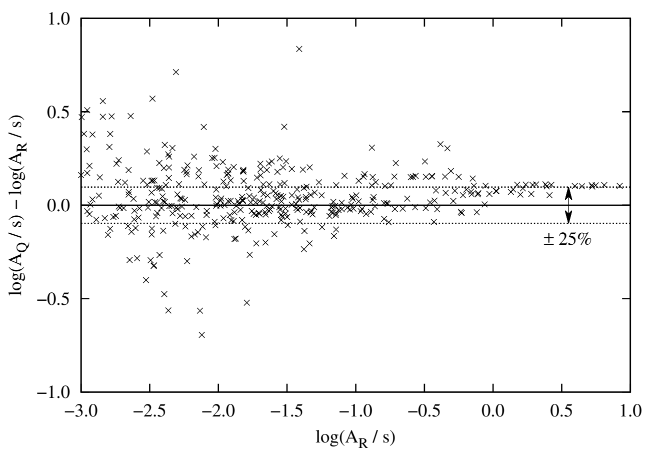

Figure 3. Comparison of calculated transition probabilities obtained by Raassen et al. (1998), A_R, with those obtained by Quinet (1998), A_Q. The dashed horizontal lines indicate differences of plus and minus 25%.

We thank M. J. Barlow, P. J. Storey, and R. L. Kurucz for helpful discussions, and the UK Science and Technology Facilities Council (STFC) for funding this research.

REFERENCES

Aldenius, M., & Johansson, S. 2007, A&A, 467, 753
Arkhipova, V. P., Klochkova, V. G., & Sokol, G. V. 2001, AstL, 27, 99
Barlow, M. J. 2012, in AIP Conf. Proc. 1438, 17th Int. Conf. Atomic Processes in Plasmas, ed. K. Aggarwal & F. Shearer (Melville, NY: AIP), 103
Birch, K. P., & Downs, M. J. 1994, Metro, 31, 315
Bönsch, G., & Potulski, E. 1998, Metro, 35, 133
Brault, J. W. 1976, JOSA, 66, 1081
Cowan, R. D., & Griffin, D. C. 1976, JOSA, 66, 1010
Fang, X., & Liu, X.-W. 2011, MNRAS, 415, 181
Hameed, S. J. 1972, JPhB, 5, 746
Hansen, J. E., Uylings, P. H. M., & Raassen, A. J. J. 1998, PhyS, 37, 664
Hartman, H., Gull, T., Johansson, S., & Smith, N. 2004, A&A, 419, 215
Kurucz, R. L. 2006a, http://kurucz.harvard.edu/atoms/2301/
Kurucz, R. L. 2006b, http://kurucz.harvard.edu/atoms/2701/
Laughlin, C. 1992, PhyS, 45, 238
Learner, R. C. M., & Thorne, A. P. 1988, JOSAB, 5, 2045
Meijerink, R., Spaans, M., & Israel, F. P. 2007, A&A, 461, 793
Norlén, G. 1973, PhyS, 8, 249
Osterbrock, G. E., & Ferland, G. J. 2006, Astrophysics of Gaseous Nebulae and Active Galactic Nuclei (2nd ed.; Sausalito, CA: Univ. Science Books)
Parpia, F. A., Froese Fischer, C., & Grant, I. P. 1996, CoPhC, 94, 249
Pickering, J. C., Raassen, A. J. J., Uylings, P. H. M., & Johansson, S. 1998, ApJS, 117, 261
Quinet, P. 1998, ApJS, 129, 147
Raassen, A. J. J., Pickering, J. C., & Uylings, P. H. M. 1998, A&AS, 130, 541
Radziemski, L. J., & Kaufman, V. 1969, JOSA, 59, 424
Smith, N., Balick, B., & Gehrz, R. D. 2005, AJ, 130, 853
Sugar, J., & Corliss, C. 1985, JPCRD, 14, 522
Thorne, A. P., Harris, C. J., Wynne-Jones, I., Learner, R. C. M., & Cox, G. 1987, JPhE, 20, 54
Thorne, A. P., Pickering, J. C., & Semeniuk, J. I. 2013, ApJS, 207, 13
Whaling, W., Anderson, W. H. C., Carle, M. T., Brault, J. W., & Zarem, H. A. 1995, JQSRT, 53, 1